

## **Molecularly engineered self-assembling membranes for cell-mediated degradation.**

Ferreira, DS; Lin, YA; Cui, H; Hubbell, JA; Reis, RL; Azevedo, HS

• "This is the peer reviewed version of the following article which has been published in final form at [10.1002/adhm.201400586]. This article may be used for non-commercial purposes in accordance with Wiley Terms and Conditions for Self-Archiving."

For additional information about this publication click this link.

<http://qmro.qmul.ac.uk/xmlui/handle/123456789/10820>

Information about this research object was correct at the time of download; we occasionally make corrections to records, please therefore check the published record when citing. For more information contact [scholarlycommunications@qmul.ac.uk](mailto:scholarlycommunications@qmul.ac.uk)

# Advanced Healthcare Materials

## Molecularly Engineered Self-assembling Membranes for Cell-mediated Degradation

--Manuscript Draft--

<b>Manuscript Number:</b>	adh.m.201400586R1
<b>Full Title:</b>	Molecularly Engineered Self-assembling Membranes for Cell-mediated Degradation
<b>Article Type:</b>	Full Paper
<b>Section/Category:</b>	
<b>Keywords:</b>	peptide amphiphiles; Hyaluronan; self-assembling membranes; matrix metalloproteinase-1; enzyme-responsive materials
<b>Corresponding Author:</b>	Helena S Azevedo, PhD Queen Mary University of London London, UNITED KINGDOM
<b>Additional Information:</b>	
<b>Question</b>	<b>Response</b>
<p>Please submit a plain text version of your cover letter here.</p> <p><b>If you are submitting a revision of your manuscript, please do not overwrite your original cover letter. There is an opportunity for you to provide your responses to the reviewers later; please do not add them here.</b></p>	<p>Dear Dr. Stimson,</p> <p>We are submitting for your consideration the paper entitled Molecularly Engineered Self-assembling Membranes for Cell-Mediated Degradation as full paper for publication in Advanced Healthcare Materials.</p> <p>This paper describes the development of self-assembling membranes that are responsive to cellular activities, in particular to hydrolytic degradation by specific enzymes. This feature is achieved by combining the matrix polymer hyaluronan and a rationally designed peptide amphiphile containing a proteolytic domain (sensitive to matrix metalloproteinase-1, MMP-1).</p> <p>The membranes were shown to be responsive to enzymes activities, in particular to hyaluronidase and MMP-1, and were completely degraded after 7 days in presence of these enzymes.</p> <p>Fibroblasts were used to assess cell-mediated degradation of the membranes and were shown to produce higher amounts of MMP-1 when cultured on MMP-sensitive membranes than when cultured on control membranes. These findings suggest that functionalized membranes stimulate protease secretion, leading to cell-mediated degradation.</p> <p>We believe this work is novel in various ways. First, the functionalization of self-assembling peptides with a MMP-1 sensitive sequence for enzyme-mediated degradation is reported for the first time in this study. Other studies have been focused in the incorporation of MMP-2 cleavable peptide, while the MMP-1 sensitive substrate has been mainly used in the functionalization of 3D polymer gels. Second, the presentation of enzymatic cleavable sequences on self-assembling membranes has never been reported. Moreover, we have designed an enzyme-responsive membrane, enabling the complete degradation of its components by cell-secreted enzymes. This is a major achievement on biomimetic design of artificial matrices for tissue engineering applications.</p> <p>Taken together, we believe that the publication of this study is timely and highly relevant to the specialized readership of Advanced Healthcare Materials.</p>
<b>Corresponding Author Secondary Information:</b>	
<b>Corresponding Author's Institution:</b>	Queen Mary University of London
<b>Corresponding Author's Secondary Institution:</b>	

<b>First Author:</b>	Daniela S. Ferreira
<b>First Author Secondary Information:</b>	
<b>Order of Authors:</b>	Daniela S. Ferreira
	Yi-An Lin
	Honggang Cui, PhD
	Jeffrey A. Hubbell, PhD
	Rui L. Reis, PhD
	Helena S Azevedo, PhD
<b>Order of Authors Secondary Information:</b>	
<b>Abstract:</b>	<p>Here we report the use of peptide engineering to develop self-assembling membranes that are responsive to hydrolytic degradation by specific enzymes. The membranes are obtained by combining hyaluronan (HA) and a rationally designed peptide amphiphile (PA) containing a proteolytic domain (GPQGIWGQ) sensitive to matrix metalloproteinase-1 (MMP-1). We found that the insertion of an octapeptide does not disturb PA self-assembly into nanofibers. In the presence of high molecular weight HA, this PA forms self-assembling membranes exhibiting a nanofibrillar morphology. Membrane enzymatic degradation was investigated in vitro in presence of hyaluronidase and MMP-1. Our studies reveal that membranes containing the MMP-1 substrate exhibit enhanced enzymatic degradation, compared with control membranes, being completely degraded after 7 days. Cell culture studies on the developed membranes, using human dermal fibroblasts (hDFBs), show that cell viability and proliferation is minimally affected by the enzymatically cleavable functionality. However, the presence of MMP-1 cleavable sequence does stimulate the secretion of MMP-1 by hDFBs and interfere with matrix deposition, particularly the deposition of collagen. By showing cell-responsiveness to biochemical signals presented on self-assembling membranes, this study highlights the ability of modulating certain cellular activities through matrix engineering.</p>

## Molecularly Engineered Self-assembling Membranes for Cell-Mediated Degradation

Daniela S. Ferreira<sup>1,2,3,6</sup>, Yi-An Lin<sup>4,5</sup>, Honggang Cui<sup>4,5</sup>, Jeffrey A. Hubbell<sup>6,7</sup>, Rui L. Reis<sup>1,2</sup>, Helena S.

Azevedo<sup>1,2,3\*</sup>

<sup>1</sup> *3B's Research Group - Biomaterials, Biodegradables and Biomimetics, University of Minho, Headquarters of the European Institute of Excellence on Tissue Engineering and Regenerative Medicine, AvePark, 4806-909 Taipas, Guimarães, Portugal*

<sup>2</sup> *ICVS/3B's - PT Government Associate Laboratory, Braga/Guimarães, Portugal*

<sup>3</sup> *School of Engineering and Materials Science, Queen Mary, University of London, Mile End Road, London, E1 4NS, UK.*

<sup>4</sup> *Department of Chemical and Biomolecular Engineering*

<sup>5</sup> *Institute for NanoBioTechnology, The Johns Hopkins University, 3400 North Charles Street, Baltimore, Maryland 21218, United States*

<sup>6</sup> *Institute for Bioengineering, School of Basic Science, École Polytechnique Fédérale de Lausanne (EPFL), Lausanne CH-1015, Switzerland*

<sup>7</sup> *Institute for Molecular Engineering, University of Chicago, Chicago, Illinois 606037, United States*

\*corresponding author: h.azevedo@qmul.ac.uk

Tel: +44(0)20 7882 5282, Fax: +44(0)20 7882 3390

### Abstract

Here we report the use of peptide engineering to develop self-assembling membranes that are responsive to cellular activities, in particular to hydrolytic degradation by specific enzymes. The membranes are obtained by combining the matrix polymer hyaluronan (HA) and a rationally designed peptide amphiphile (PA) containing a proteolytic domain (GPQGIWGQ octapeptide) sensitive to matrix metalloproteinase-1 (MMP-1). The self-assembly behavior of the designed MMP-1 sensitive PA was studied by circular dichroism (CD) spectroscopy, transmission electron microscopy (TEM) and ability to form membranes with HA. We found that the insertion of an

1 octapeptide in a typical PA structure does not disturb its self-assembly process into fibrillar  
2 nanostructures. CD shows the formation of  $\beta$ -sheet secondary structures in a broad pH range and  
3 TEM reveals the presence of filamentous nanostructures. In the presence of high molecular weight  
4 HA, this PA forms self-assembling membranes exhibiting a nanofibrillar morphology. Membrane  
5 enzymatic degradation was then investigated *in vitro* in presence of exogenous enzymes  
6 (hyaluronidase and MMP-1). Our studies reveal that membranes containing the MMP-1 substrate  
7 exhibit enhanced enzymatic degradation, compared with control membranes (absence of MMP-1  
8 cleavable peptide or containing a MMP-1 insensitive sequence), being completely degraded after  
9 7 days. Cell culture studies on the developed membranes, using human dermal fibroblasts (hDFbs),  
10 show that cell viability and proliferation is minimally affected by the enzymatically cleavable  
11 functionality present on the membrane. However, the presence of MMP-1 cleavable sequence  
12 does stimulate the secretion of MMP-1 by hDFbs and interfere with matrix deposition, particularly  
13 the deposition of collagen. By showing cell-responsiveness to biochemical signals presented on  
14 self-assembling membranes, this study highlights the ability of modulating certain cellular  
15 activities through matrix engineering. We believe this concept can be further explored to  
16 understand the cellular remodeling process in different tissues and could also be used as a  
17 strategy to develop artificial matrices with more biomimetic degradation for tissue engineering  
18 applications.  
19  
20  
21  
22  
23  
24  
25  
26  
27  
28  
29  
30  
31  
32

33  
34  
35  
36 **Keywords:** peptide amphiphiles; hyaluronan; self-assembling membranes; matrix  
37 metalloproteinase-1; degradation; enzyme-responsive materials  
38  
39  
40  
41  
42  
43  
44  
45  
46  
47  
48  
49  
50  
51  
52  
53  
54  
55  
56  
57  
58  
59  
60  
61  
62  
63  
64  
65

## 1. Introduction

1 The specific and selective activities of enzymes, together with their ability to be controlled by  
2  
3 environmental conditions, such as pH, temperature and ionic strength, have been extensively  
4  
5 explored in the materials science community with the aim of producing materials with customized  
6  
7 functionalities while offering the possibility to perform catalysis reactions very efficiently in mild  
8  
9 conditions. According to a recent review published by Ulijn and co-workers on enzyme responsive  
10  
11 materials (ERMs),<sup>[1]</sup> they define ERMs as materials that change their functionality as a result of the  
12  
13 direct action of an enzyme on the material. The ubiquitous distribution and great diversity of  
14  
15 enzymes present in the human body has motivated biomedical engineers to design biomaterials  
16  
17 responsive to enzyme activities and thus translate the enzymatic modification into a suitable  
18  
19 materials response. Because the trigger is provided by the biological environment (e.g. cells), with  
20  
21 no need to be added exogenously, ERMs offer additional advantages for biomedical applications  
22  
23 when compared with other stimuli-responsive (e.g. light, temperature) materials. Enzymes can  
24  
25 either be used to form new covalent bonds (e.g. isopeptide bonds between side groups of amino  
26  
27 acids in peptides and proteins by transglutaminase, leading to the cross-linking and strengthening  
28  
29 of the material), or the cleavage of pre-existing bonds (e.g. hydrolysis of peptide bonds by  
30  
31 proteases, leading to the material degradation or disassembly). In the context of 3D biomaterials  
32  
33 for cell culture, enzymes have been mainly used to form polymer hydrogels, by incorporating  
34  
35 enzyme sensitive cross-links and thus induce gelation *in vivo*, or, conversely, to mimic the  
36  
37 degradation process during tissue remodeling and favor cell migration and invasion through  
38  
39 enzyme sensitive polymer hydrogels. Both approaches were pioneered by the Hubbell's lab to  
40  
41 develop polyethylene glycol (PEG)-based hydrogels with different functionalities.<sup>[2, 3]</sup> These  
42  
43 concepts were then applied to other natural<sup>[4, 5]</sup> and synthetic<sup>[6]</sup> polymer hydrogels. Similarly,  
44  
45 enzyme responsive supramolecular hydrogels were developed, including the formation of gels that  
46  
47 are obtained<sup>[7]</sup> by enzyme-directed self-assembly<sup>[7]</sup> (an enzyme is used to catalyze the synthesis of  
48  
49  
50  
51  
52  
53  
54  
55  
56  
57  
58  
59  
60  
61  
62  
63  
64  
65

self-assembling molecules or the removal of a block to trigger the self-assembly), and the degradation<sup>[8,9,10]</sup> of supramolecular gels by enzyme mediated disassembly (enzyme converts the self-assembling blocks into non-self-assembling molecules or by degrading the building block directly).<sup>[1]</sup> Selective enzymatic degradation was also shown to be advantageous in modulating the properties of self-assembled nanostructures, such as nanostructure transitions. For example, Webber and co-workers designed a peptide amphiphile (PA) containing a sequence that is a substrate of a protein kinase A (PKA).<sup>[11]</sup> Upon treatment with PKA, the PA molecules became phosphorylated causing the disassembly of the original cylindrical structures. Subsequent treatment with alkaline phosphatase enzyme, which cleaves the phosphate groups, resulted in PA reassembly. Seitsonen and co-workers used the model protease  $\alpha$ -chymotrypsin to control the morphologies of peptide self-assemblies (nanotubes/helical ribbons, spherical micelles).<sup>[12]</sup> In a different approach, Lin and co-workers used a specific proteinase to degrade a cross-linker that stabilizes supramolecular peptide filaments.<sup>[13]</sup>

Normally during granulation tissue formation, the remodeling of the natural extracellular matrix (ECM) occurs simultaneously with cell invasion. The macromolecular components of the ECM are degraded by cell-secreted proteases, mainly by matrix metalloproteinases (MMPs). The MMPs are a family of protease enzymes that are able to cleave structural components of the ECM, such as collagen types I and IV and fibrin, playing an important role in morphogenesis, wound healing and tissue remodeling.<sup>[14]</sup> In general, MMPs are not continuously expressed in the skin, but are induced temporarily in response to exogenous signals or pathogenic conditions, such as wound healing.<sup>[15]</sup> In later stages of dermal wound healing, fibroblasts are the main cell population that produce native ECM<sup>[16]</sup> and secrete active MMPs (MMP-1, -2, -9 and -13).<sup>[15,17]</sup> The action of MMP-1 is essential in the remodeling stage during wound healing.<sup>[18]</sup> This enzyme is an antagonist to the ECM synthesis and therefore mediates the balance between tissue synthesis and degradation. Several attempts in biomaterial design have been made to mimic this feature of natural ECMs by

1 including protease-sensitive peptides that are cleaved in the presence of cell-secreted enzymes,  
2 thus providing further control over cellular responses.<sup>[2, 19]</sup> The inclusion of MMP-sensitive  
3 sequences into PEG gels has been explored by Hubbell's lab to promote cell migration within  
4 hydrogels.<sup>[2, 20, 21]</sup> When the gels come into contact with cells *in vitro* or *in vivo*, they were locally  
5 degraded as the cells respond to cues presented by the gels. The inclusion of MMP cleavable  
6 sequences into self-assembling peptides has been explored for different biomedical applications,  
7 including enzyme responsive hydrogels for controlled matrix degradation and cell migration in  
8 tissue engineering,<sup>[8, 9, 22]</sup> enzyme-triggered drug delivery systems<sup>[23]</sup> and sensing systems for  
9 detecting cell-secreted MMPs overexpressed in various diseases.<sup>[24]</sup>

10 Hyaluronan (HA), a major component of the ECM, has attracted considerable interest in a wide  
11 range of biomaterials applications.<sup>[25]</sup> Its unique physicochemical properties<sup>[26]</sup> (high molecular  
12 weight and density of negative charges, inherent biodegradability and biocompatibility),  
13 associated with its complex interactions with ECM components and cells,<sup>[27]</sup> have led us and others  
14 to consider this simple polymer as building block for designing biomimetic materials. Moreover,  
15 HA has shown to play important roles in wound healing.<sup>[28]</sup>

16 As bottom-up approach, self-assembly allows the design of biomaterials with specific  
17 functionalities and nanoscale organization similar to natural tissues. The formation of  
18 hierarchically ordered membranes by self-assembly between high molecular weight HA and  
19 positively charged peptide amphiphiles (PAs) was first reported in the seminal work of Stupp and  
20 co-workers.<sup>[29]</sup> We have then used the same approach to fabricate membranes integrating  
21 biochemical signals (RGDS ligand) to enhance the adhesion of fibroblasts in serum-free culture  
22 conditions.<sup>[30]</sup> To further expand the versatility of these self-assembling membranes as temporary  
23 matrices for wound healing applications, and recreate some of the aspects of matrix remodeling,  
24 an enzymatic cleavable peptide sequence has now been included into the peptide domain. The



inclusion of this sequence allows the creation of membranes that are degraded in response to cell-secreted enzyme activities at the wound site during tissue remodeling.

Therefore, the objective of this study was to develop self-assembling membranes made of HA and PAs containing a cleavable site for MMP-1. Since hyaluronidase and MMP-1 enzymes are released by fibroblasts during wound healing, we further examined the ability of these enzymes to degrade the self-assembling membranes. The biological functionality of the membranes was also investigated by culturing human dermal fibroblasts and their effect on cell behavior, like cell adhesion, proliferation and ECM synthesis, evaluated.

## 2. Results and discussion

### 2.1. Design and self-assembly of PAs with enzymatic cleavable sequences

The self-assembly of HA with positively charged peptides containing the RGDS epitope has previously been explored by our group to generate membranes with different densities of peptide ligands and thus control the adhesion of different cell types.<sup>[30, 31]</sup> To add different functionalities into our membrane design, such as programmed degradation, a similar molecular engineering approach was pursued in this work by including the matrix metalloproteinase-1 (MMP-1) cleavable site into the peptide building block. The peptide self-assembling blocks used in this study are based on the peptide amphiphile design pioneered by Stupp<sup>[32]</sup> and are composed of a hydrophobic segment coupled to a peptide segment, that includes a  $\beta$ -sheet forming sequence ( $V_3A_3$ ) and a domain with positively charged amino acids ( $K_3$ ) to bind the anionic HA ( $K_3$  PA, Figure 1A).<sup>[29]</sup> A MMP-1-sensitive PA was designed by incorporating the sequence GPQG↓IWGQ<sup>[2, 20, 21, 33]</sup> (arrow denotes the expected cleavage site by MMP-1) between the  $\beta$ -sheet domain and the lysine residues (MMP<sub>s</sub> $K_3$  PA, MMP sensitive). This peptide is the mutated version of the sequence GPQG↓IAGQ found within the  $\alpha$  chain of type I collagen of calf and chick, as well as human.<sup>[34]</sup> The single substitution of Ala by Trp was shown to enhance enzymatic cleavage.<sup>[2, 35]</sup> The human  $\alpha 1$  type IV collagen sequence, GDQGIAGF, was chosen as a negative control. This sequence has been described to be insensitive to MMP-1 degradation (MMP<sub>i</sub> $K_3$  PA, MMP insensitive).<sup>[2, 36]</sup> By inserting the GPQG↓IWGQ segment between the HA-binding region and the  $\beta$ -sheet forming segment in the original PA design, instead of adding it to the C-terminus, we aim to promote the breakdown of the peptide at a point that would facilitate the release of the HA-binding motif from the PA nanofibers, hindering **binding to** HA to remain bound. The lack of interaction between the PA nanofibers and the HA chains would favor the disassembly and dissolution of the membrane components. In addition to MMP-1, hyaluronidase (HAase) has also been implicated in tissue remodeling during wound healing. The presence of HAase will further contribute for the

1 membrane disassembly and degradation by hydrolyzing HA into smaller fragments.<sup>[30]</sup> We  
2 hypothesize that the incorporation of enzymatic cleavable building blocks in the formulation of  
3 our membranes, enables the complete degradation of its components by cell-secreted enzymes  
4 and this process would resemble the breakdown of native ECM during tissue remodeling.  
5  
6 The ability of K<sub>3</sub>-PA to form  $\beta$ -sheet secondary structures at certain pHs and to self-assemble into  
7 nanofibers was shown previously.<sup>[30]</sup> However, significant modifications, like the insertion of a  
8 sequence containing eight amino acids, may affect the self-assembly properties of the resulting  
9 PAs. Profiling the secondary structure of the GPQGIWGQ-containing PA by CD spectroscopy and  
10 examining the existence of  $\beta$ -sheets can provide basic information to understand their assembling  
11 properties (Figure 1B). The CD spectra of  $\beta$ -sheet structures are typically characterized by a  
12 minimum at 216 nm and a maximum at 195 nm, while random coils present a maximum at 218 nm  
13 and a minimum at 198 nm.<sup>[37]</sup> The CD spectra obtained for K<sub>3</sub>PA at neutral and basic pH were  
14 consistent with the known fact that this peptide has a dominant  $\beta$ -sheet content.<sup>[30, 38]</sup> The  
15 inclusion of the sequences GPGIWGQ and GDQGIAGF between the  $\beta$ -sheet domain and the  
16 positively charged lysine residues seems to reinforce the  $\beta$ -sheet behavior of the peptides (Figure  
17 1B). A typical  $\beta$ -sheet signature was observed for both peptides in all the studied pH conditions,  
18 with a minimum in the 210-220 nm range, a crossover from positive to negative above 190 nm,  
19 and a positive ellipticity around 200 nm (Figure 1B). With exception of proline, all the inserted  
20 amino acids are either neutral or  $\beta$ -sheet promoters,<sup>[39]</sup> thus contributing to the formation of  $\beta$ -  
21 sheet structures, independently of the solution pH.  
22  
23 PAs, including these designed in this study, typically self-assemble into high-aspect-ratio  
24 filamentous nanostructures. TEM analysis (Figure 1C) confirmed the self-assembly of all PAs into  
25 nanofiber structures with diameters of between 12 and 16 nm (Table S1) and lengths of from a  
26 few hundred nanometers to several micrometers. Interestingly, MMP<sub>5</sub>K<sub>3</sub> PA formed shorter  
27 nanofibers in comparison with K<sub>3</sub> and MMP<sub>1</sub>K<sub>3</sub> PAs. This might be due to the placement of a proline

residue next to the  $\beta$ -sheet forming peptide region. The cyclic structure of proline's side chain confers exceptional conformation rigidity. Its unique kink formation may add some steric effect on the molecular packing of the adjacent residues, thus limiting the growth of the nanofiber.

## 2.2. Membrane self-assembly

Recent advances in biomaterials science have enabled the possibility to develop artificial matrices that recapitulate key features of the natural ECM critical for the process of tissue regeneration.<sup>[40]</sup>

Based on our previous studies,<sup>[30]</sup> we hypothesize that self-assembling membranes with diverse functionalities can be obtained by self-assembly between HA and positively charged PAs through the incorporation of specific sequences recognized by cell receptors or specific enzymes (Figure 1A). Although the insertion of a sequence of eight amino acids into the PA structure did not disturb their self-assembly properties (Figure 1B, 1C) the presence of this additional segment could potentially affect the membrane self-assembly. To prepare the membranes (Figure S4), an aqueous solution containing K<sub>3</sub> PA was added on the top of the HA solution, and left to incubate overnight at the temperature of 37 °C. Similarly, membranes containing the MMP-sensitive (Figure S5) and -insensitive sequences were prepared using MMP<sub>3</sub>K<sub>3</sub> PA and MMP<sub>1</sub>K<sub>3</sub> PA, respectively. SEM images (Figure 3B1) showed that all membranes present a nanofibrillar structure that resulted from the PA self-assembly in presence of the anionic polysaccharide.

## 2.3. Membrane degradation by exogenous enzymes

Various studies<sup>[4,21]</sup> have showed that non-degradable hydrogels limit cellular infiltration. We have demonstrated that self-assembling membranes containing HA and K<sub>3</sub> PA were susceptible to enzymatic degradation by HAase.<sup>[30]</sup> The incorporation of MMP-sensitive sequences in our membrane design is expected to promote their degradation by proteolytic enzymes and this would lead to enhanced cellular invasion (Figure 2). Thus, when implanted *in vivo* both

1 components of the membrane would be susceptible to degradation by enzymes expressed by the  
2 surrounding cells (e.g. HAase, MMPs) improving cell migration and tissue morphogenesis.

3  
4 To assess membrane degradability, membranes containing the MMP sensitive sequence (MMP<sub>5</sub>K<sub>3</sub>-  
5 HA), the insensitive sequence (MMP<sub>1</sub>K<sub>3</sub>-HA) and the control (K<sub>3</sub>-HA) were incubated in PBS in the  
6 presence of HAase (50 U mL<sup>-1</sup>), MMP-1 (10 nM) or both enzymes. HA degradation was followed by  
7  
8  
9  
10  
11  
12  
13  
14  
15  
16  
17  
18  
19  
20  
21  
22  
23  
24  
25  
26  
27  
28  
29  
30  
31  
32  
33  
34  
35  
36  
37  
38  
39  
40  
41  
42  
43  
44  
45  
46  
47  
48  
49  
50  
51  
52  
53  
54  
55  
56  
57  
58  
59  
60  
61  
62  
63  
64  
65

quantification of a new reducing N-acetyl-D-glucosamine terminus with each cleavage reaction and membranes were analyzed by SEM (Figure 3). Incubation in PBS up to 14 days did not cause degradation of the membranes, as evidenced by the low amount of N-acetylamino sugars in the supernatants (Figure 3A1, A2), and the absence of evident signs of degradation in the SEM micrographs (Figure 3B1). When incubated in the presence of HAase, membrane degradation was significantly enhanced in all the conditions, which is in agreement with what we have observed before.<sup>[30]</sup> In the presence of MMP-1, only the MMP<sub>5</sub>K<sub>3</sub>-HA membranes showed signs of degradation, as seen in the SEM micrographs (Figure 3B1). From day 5, there is a slightly increase in the released N-acetylamino sugars (Figure 3A2). Analyzing the effect of MMP-1 activity on the release of N-acetylamino sugars from MMP<sub>5</sub>K<sub>3</sub>-HA and MMP<sub>1</sub>K<sub>3</sub>-HA membranes (Figure 3A3), only the MMP<sub>5</sub>K<sub>3</sub>-HA membranes showed an increase in the amount of N-acetylamino sugars in solution, while in the MMP<sub>1</sub>K<sub>3</sub>-HA the amount of N-acetylamino sugars was negligible and remained constant along the time. The increase in the amount of N-acetylamino sugars in solution might be due to the release of HA from the membrane, as the peptide being cleaved by MMP-1 (it breaks down the HA-binding region from the main PA sequence) weakens the interaction with HA. The absence of degradation in the K<sub>3</sub>-HA and MMP<sub>1</sub>K<sub>3</sub>-HA membranes in the presence of MMP-1 suggests the specificity of the enzyme for the MMP substrate (GPQG↓IWGQ) and that the control sequence (GDQGIAGF) is not cleaved by the enzymatic actions of MMPs, as reported previously.<sup>[2]</sup> In the presence of both HAase and MMP-1, the MMP<sub>5</sub>K<sub>3</sub>-HA membranes were completely degraded after 14 days, demonstrating the additive effect of both enzymes. At this stage,

1 membranes underwent extensive degradation and were difficult to recover for SEM analysis, thus  
2 SEM micrograph shows a sample only for day 7 (Figure 3B1). SEM analysis of the cross-section of  
3  
4 MMP<sub>5</sub>K<sub>3</sub>-HA membranes in the presence of MMP-1, shows that the degradation was more evident  
5  
6 on the surface on the peptide side (Figure 3B2).  
7  
8  
9

## 10 11 **2.4. Cell culture studies**

### 12 ***Effect of membrane functionalization on fibroblast proliferation***

13  
14 During the early stages of wound healing, fibroblast migration and proliferation into the wound  
15  
16 matrix depend on cell-matrix interactions.<sup>[18, 41]</sup> Previous work suggested that PAs bearing  
17  
18 different charges could affect cell viability.<sup>[42]</sup> To investigate whether some of the sequences could  
19  
20 affect fibroblast viability and proliferation, cells were cultured either on glass coverslips coated  
21  
22 with different PA molecules or on membranes made with HA and the same PAs. Moreover, the  
23  
24 effect of the addition of a broad-spectrum MMP inhibitor (GM6001) in cell proliferation was also  
25  
26 investigated, as we intend to use this inhibitor in further experiments. DNA quantification results  
27  
28 showed that cells were able to proliferate up to 7 days, either on glass coated coverslips (Figure  
29  
30 S4) or on the membranes (Figure 4), which indicates that these PA molecules do not affect cell  
31  
32 proliferation. Additionally, cell proliferation was greatly decreased in the presence of the MMP-  
33  
34 inhibitor (GM6001, 20 μM), which is consistent with what has been observed by other authors  
35  
36 that suggest this inhibitor might have a reversible effect on fibroblast proliferation.<sup>[21, 43]</sup> Contrary  
37  
38 to what has been observed when culturing cells in 3D hydrogels,<sup>[9, 21]</sup> there was no difference on  
39  
40 cell proliferation when cells were seeded on MMP<sub>5</sub>K<sub>3</sub>-HA membranes versus MMP<sub>1</sub>K<sub>3</sub>-HA.  
41  
42  
43  
44  
45  
46  
47  
48  
49  
50  
51  
52  
53  
54

### 55 ***Effect of membrane functionalization on MMP-1 secretion by fibroblasts***

56  
57 In later stages of dermal wound healing, fibroblasts are the main cell population that produces  
58  
59 native ECM.<sup>[16]</sup> Cells normally secrete and activate proteolytic enzymes in order to invade or  
60  
61  
62  
63  
64  
65

remodel the extracellular microenvironment.<sup>[44]</sup> In particular, primary human dermal fibroblasts are known to secrete active MMPs.<sup>[17]</sup> At this stage, for successful wound healing and prevention of fibrotic tissue, a fine balance between ECM synthesis and degradation is required. The action of MMP-1 is essential during the remodeling stage of wound healing.<sup>[18]</sup> Here, MMP-1 expression was examined at the protein level using ELISA. Fibroblasts cultured on the membranes were shown to secrete MMP-1. The amounts of MMP-1 released by the cells cultured on the MMP<sub>5</sub>K<sub>3</sub>-HA membranes were higher than those of cells cultured on the corresponding MMP-insensitive derivatives and on the control (K<sub>3</sub>-HA) (Figure 5A), suggesting that the presence of MMP-sensitive motifs in the membrane might have an influence in the secretion of MMP-1. When cultured on peptide coated glass coverslips, however, no differences were observed between different PAs on MMP-1 production (Figure S7). In addition, the values for MMP<sub>5</sub>K<sub>3</sub>-HA membranes were 2-fold higher than on the coated glass. These findings suggest that the mode of signal presentation to cells may have an influence on their response, a hypothesis that remains to be further investigated. Previous studies have shown the influence of matrices presenting bioactive ligands on the secretion of proteases.<sup>[2, 4]</sup> As expected, small amount of MMP-1 was detected in the supernatant in the presence of the MMP-inhibitor (Figure 5A). Confocal microscopy images showed elongated cells with typical fibroblast morphology (Figure 5B). After 24 h, MMP-1 was expressed by the cells in all the conditions but seems more evident for MMP<sub>5</sub>K<sub>3</sub>-HA membranes, which corroborates the ELISA results (Figure 5A).

### ***Production of ECM proteins by fibroblasts cultured on the membranes with different functionalities***

The native ECM of the dermis mainly consists of collagens, proteoglycans and adhesive glycoproteins.<sup>[45]</sup> In wound healing, fibroblasts are essential for the production of new native ECM.<sup>[46]</sup> To investigate the ability of hDFBs to synthesize native ECM, we determined the amount

of collagen and non-collagenous extracellular matrix proteins produced by the cells when cultured on the different membranes (Figure 6). Except for the MMP<sub>5</sub>K<sub>3</sub>-HA membranes, there was an increase in collagen and non-collagenous proteins production with culture time in all the conditions. The amount of collagen deposited on MMP<sub>5</sub>K<sub>3</sub>-HA membranes decreased with time (Figure 6A) while the amount of non-collagenous proteins increased, as observed for the other conditions (Figure 6B). The ECM turnover is controlled by the synthetic rate of matrix proteins, including collagenous and non-collagenous proteins, and their enzymatic degradation by MMPs. In particular, MMP-1 is the only protease able to unwind collagen type I and initiate its degradation.<sup>[47]</sup> Elevated MMP-1 activity is responsible for an increased turnover of the extracellular collagen matrix.<sup>[48]</sup> Taken together, the data of collagen and MMP-1 production, suggest that the reduced levels of collagen on MMP<sub>5</sub>K<sub>3</sub>-HA membranes (Figure 6A) could be due to the increased amounts of secreted MMP-1 (Figure 5A) observed for these membranes. As previously observed for the production of MMP-1, no differences were shown between conditions on the production of collagen when cells were cultured on peptide coated glass coverslips (Figure S8A), suggesting again the effect of matrix microarchitecture and signal presentation on cell behavior.

### ***Membrane microstructure after cell culture***

SEM analysis of the membranes after culturing hDFBs showed that cells were able to adhere to and invade the membranes (Figure 7). After 14 days of culture, the microstructure of the MMP-sensitive membranes showed a loose network of nanofibers, when compared with the control membranes (K<sub>3</sub> and MMP<sub>insensitive</sub>). Conversely, when adding the MMP inhibitor into the culture medium, the membrane retained its initial morphology. These results suggest that the underlying membrane is responsive to the enzymatic activities produced by the cells. However, the membranes remained intact after 14 days, implying that cell-triggered proteolysis was localized on



1 the surface of the membranes into the cell periphery. The localization of the enzymatic  
2 degradation on the surface mimics proteolysis *in vivo*, in which ECM degradation is confined to the  
3 immediate pericellular environment.<sup>[44]</sup> An adequate correlation between the membrane  
4 degradation and production of MMP-1 is not possible at this point, because other MMPs are  
5 secreted by fibroblasts (MMP-2, MMP-13). In addition, a balance between active MMPs and their  
6 natural inhibitors (tissue inhibitors of metalloproteinases, TIMPs) could also be responsible for the  
7 localized degradation behavior in the membranes. Thus, we cannot conclude at the moment  
8 which particular molecules are involved in cell proteolysis, but we have an indication that at least  
9 MMP-1 is involved.

10  
11 The balanced regulation of fibroblast proliferation and ECM remodeling is essential for optimal  
12 wound healing results. Our *in vitro* data suggest that cells responded to the functionalized  
13 membranes, and were able to produce ECM proteins without extensive matrix deposition. The  
14 inclusion of a MMP-sensitive sequence into the membranes increased matrix proteolytic  
15 degradability, which would lead to enhanced cellular invasion when implanted *in vivo*, and thus  
16 could be beneficial for an enhanced wound healing response. The mechanisms underlying these  
17 observations remain, however, unclear and are worthy to be further investigated.

### 3. Conclusions

1 Using a molecular engineering approach, we designed a peptide amphiphile capable of self-  
2  
3 assembling with hyaluronan into membranes and containing a proteolytic domain sensitive to  
4  
5 matrix metalloproteinase-1 (MMP-1). By pursuing this design, we were able to modulate the  
6  
7 degradation rate of the formed self-assembling membranes, as well as certain cellular responses.  
8  
9 The membranes were shown to be responsive to enzymes activities, in particular to hyaluronidase  
10  
11 and MMP-1, and were completely degraded after 7 days in presence of exogenous enzymes.  
12  
13 Fibroblasts, very active cells in the wound healing process, were used to assess cell-mediated  
14  
15 degradation of the membranes and were shown to produce higher amounts of MMP-1 when  
16  
17 cultured on MMP-sensitive membranes than when cultured on the MMP-insensitive and on the  
18  
19 control (bare membranes without MMP signal). These findings suggest that membranes  
20  
21 containing the MMP-1 cleavable sequence stimulate protease secretion, thus leading to cell-  
22  
23 mediated degradation process. This hypothesis, however, needs to be further investigated. We  
24  
25 expect that by including components sensitive to enzymatic activities in the membrane  
26  
27 formulation, their degradation behavior may resemble the process of ECM remodeling, leading to  
28  
29 increased cellular infiltration and ultimately more robust healing *in vivo*. Nevertheless, *in vivo*  
30  
31 experiments will still be required to verify that the expected remodeling of the ECM actually takes  
32  
33 place. These cell-interactive membranes can be further functionalized with other biochemical  
34  
35 moieties to study cellular processes *in vitro* and also as temporary matrices in tissue engineering  
36  
37 applications.  
38  
39  
40  
41  
42  
43  
44  
45  
46  
47  
48  
49  
50  
51  
52

### Acknowledgments

53 This work was funded by the European Regional Development Fund (ERDF) through the  
54  
55 Operational Competitiveness Programme "COMPETE" (FCOMP-01-0124-FEDER-014758) and  
56  
57 national funds through the Portuguese Foundation for Science and Technology (FCT) under the  
58  
59  
60  
61  
62  
63  
64  
65

project PTDC/EBB-BIO/114523/2009. We also thank a start-up grant provided by the School of Engineering and Materials Science at QMUL. D. S. Ferreira gratefully acknowledges FCT for the PhD scholarship (SFRH/BD/44977/2008).

1  
2  
3  
4  
5  
6  
7  
8  
9  
10  
11  
12  
13  
14  
15  
16  
17  
18  
19  
20  
21  
22  
23  
24  
25  
26  
27  
28  
29  
30  
31  
32  
33  
34  
35  
36  
37  
38  
39  
40  
41  
42  
43  
44  
45  
46  
47  
48  
49  
50  
51  
52  
53  
54  
55  
56  
57  
58  
59  
60  
61  
62  
63  
64  
65

## 4. Experimental Section

### Hyaluronan (HA)

Hyaluronan, with an average molar mass of 1.5 MDa (Lifecore Biomedical, Inc, Chaska, USA) was used in this study for self-assembly with the newly designed peptide amphiphiles.

### Peptide amphiphiles: design/structure, synthesis and purification

Three different peptide amphiphiles (PAs) were synthesized in this work, all consisting of a peptide segment covalently linked to a 16-carbon alkyl chain:  $C_{15}H_{31}CO-V_3A_3K_3$  ( $K_3$  PA),  $C_{15}H_{31}CO-V_3A_3GPQGIWGQK_3$  ( $MMP_5K_3$  PA) and  $C_{15}H_{31}CO-V_3A_3GDQGIAGFK_3$  ( $MMP_iK_3$  PA) (Figure 1A). The peptides were synthesized on a CS Bio 136XT automated peptide synthesizer (CS Bio, USA) using standard 9-fluorenylmethoxycarbonyl (Fmoc) based solid phase chemistry on a 4-methylbenzhydrylamine (MBHA) rink amide resin. Amino acid couplings were performed using 4 equivalents (4 mmol) of Fmoc protected amino acids (Novabiochem, USA), 4 equivalents of O-(Benzotriazol-1-yl)-N,N,N',N'-tetramethyluronium hexafluorophosphate (HBTU, Carbosynth, UK) and 6 equivalents of N,N-diisopropylethylamine (DIEA, Sigma, USA). Fmoc deprotections were performed with 20% piperidine (Sigma, USA) in dimethylformamide. A palmitic acid ( $C_{16}H_{32}O_2$ , Calbiochem, USA) tail was manually coupled under the same conditions as the Fmoc-amino acids. Peptide cleavage from the resin, and removal of the protecting groups, was carried out on a mixture of trifluoroacetic acid (TFA, Sigma, USA)/triisopropylsilane (TIS, Alfa Aesar)/water (95/2.5/2.5) for 3 h at room temperature. The peptide mixture was collected and excess of TFA was removed by rotary evaporation. The resulting viscous peptide solution was triturated with cold diethyl ether and the white precipitate was collected by filtration, washed with cold ether, and allowed to dry under vacuum overnight. The peptide mass was confirmed by electrospray ionization mass spectrometry (ESI-MS, Agilent, USA).

1 Peptides were then purified on a Waters 2545 Binary Gradient high-performance liquid  
2 chromatography (HPLC) system using a preparative reverse-phase C18 column (Atlantis Prep OBD  
3 T3 Column, Waters, USA) and a water/acetonitrile (0.1% TFA) gradient. TFA counter-ions were  
4 exchanged by sublimation from 0.01 M hydrochloric acid. Finally, the peptides were dialyzed  
5 against ultrapure water using 500 MWCO dialysis tubing (Spectrum labs, The Netherlands),  
6 lyophilized and stored at -20 °C until further use. Confirmation of mass and purity was done by ESI-  
7 MS and HPLC (Supplementary Information, Figure S1-S3).  
8  
9  
10  
11  
12  
13  
14  
15  
16  
17  
18

## 19 **Peptide amphiphiles characterization**

### 20 ***Circular dichroism (CD) spectroscopy***

21 Peptides were dissolved in deionized water to a final concentration of 0.011 mM and the pH was  
22 adjusted to 3, 7 and 9 with hydrochloric acid (0.1 M) or ammonium hydroxide (0.1 M). The CD  
23 measurements were performed in a PiStar-180 spectrometer from Applied Photophysics (Surrey,  
24 UK), under a constant flow of nitrogen (8 L.min<sup>-1</sup>) at a constant pressure value of 0.7 MPa. Far-UV  
25 spectra were recorded at 25 °C from 190 to 300 nm in a quartz cuvette with 1 mm path-length. All  
26 scans were performed in the steady state with a bandwidth of 1 nm and each represented  
27 spectrum is an average of 5 spectra. The molar ellipticity  $[\theta]$  was calculated using equation (1).  
28  
29  
30  
31  
32  
33  
34  
35  
36  
37  
38  
39  
40  
41

$$42 \quad [\theta] = \frac{\theta}{c.l} \quad (1)$$

43 were  $\theta$  is the measured ellipticity in mdeg,  $c$  is the concentration of the peptide in  $\text{dmol L}^{-1}$  and  $l$  is  
44 the light path length of the cuvette in cm.  
45  
46  
47  
48  
49  
50  
51  
52

### 53 ***Transmission electron microscopy (TEM)***

54 Peptides were dissolved in ultrapure water (0.1 wt%) and the solution was aged for 2 days before  
55 TEM analysis. Peptide solutions were loaded on carbon-coated copper TEM grid (Electron  
56  
57  
58  
59  
60  
61  
62  
63  
64  
65

Microscopy Sciences, USA). For negative staining, a drop of 2 wt% uranyl acetate (Electron Microscopy Sciences, USA) aqueous solution was placed on the samples. The excess solution was wiped away by a piece of filter paper, and the sample was allowed to dry under ambient conditions. All images were collected with a Tecnai 12 TWIN, equipped with SIS Megaview III camera (FEI, USA).

### **Preparation of self-assembled PA-HA membranes containing different functionalities**

Self-assembled membranes were prepared by combining HA with positively charged PAs at optimized conditions, as previously reported.<sup>[30]</sup> Briefly, 50  $\mu\text{L}$  of a 1 wt% HA solution was cast on the bottom of the wells of a 96 well plate and then 50  $\mu\text{L}$  of 0.017 M  $\text{K}_3\text{PA}$  solution was added on top of the HA solution. Similarly, membranes containing the MMP sensitive and insensitive sequences were prepared using  $\text{MMP}_s\text{K}_3$  and  $\text{MMP}_i\text{K}_3$  PAs at 0.017 M concentration. The membranes were allowed to develop overnight and rinsed with sterile ultrapure water to ensure the removal of unreacted HA and PA.

### ***Enzymatic degradation of PA-HA membranes by exogenous enzymes (MMP-1 and hyaluronidase)***

Degradation studies were carried out by incubating the different PA-HA membranes in PBS at 37  $^{\circ}\text{C}$  for 14 days without enzymes (control) or containing 10 nM of MMP-1 (human MMP-1, EC 3.4.24.7, Sigma, USA) and 50  $\text{U}\cdot\text{mL}^{-1}$  of bovine testicular hyaluronidase (Type IV, EC 3.2.1.35, Sigma, USA) isolated or combined. The enzyme solutions were replaced every 72 h throughout the study and collected supernatants were stored at -20  $^{\circ}\text{C}$  for further analysis. At predetermined time points, the membranes were collected and their morphology examined by SEM, as described below. HA degradation on the membranes was assessed by quantification of N-acetylamino sugars in the collected supernatants using the fluorimetric Morgan–Elson assay method<sup>[49]</sup> and a

1 calibration curve of N-acetyl-D-glucosamine (NAG) standards. Three independent experiments  
2 were performed for each degradation condition and incubation time.  
3  
4  
5

### 6 **Scanning electron microscopy (SEM)**

7

8 The microstructure of the membranes after degradation was analyzed by SEM. The membranes  
9 were first fixed in 2% glutaraldehyde/3% sucrose in PBS for 1 h at 4 °C followed by sequential  
10 dehydration in graded ethanol concentrations (from 20 to 100%). To remove ethanol, samples  
11 were dried in a critical point dryer (Tousimis Autosandri®-815 series A, USA). Prior observation, the  
12 samples were coated with a 15 nm thick layer of gold/palladium and imaged using an ultra-high  
13 resolution field emission gun scanning electron microscope (Nova™ NanoSEM 200) from FEI  
14 (Eindhoven, The Netherlands).  
15  
16  
17  
18  
19  
20  
21  
22  
23  
24  
25  
26  
27  
28

### 29 **Cell culture studies**

30

#### 31 **Isolation and culture of primary human dermal fibroblasts (hDFbs)**

32  
33

34 hDFbs were isolated from skin samples discarded from abdominoplasty surgeries of consenting  
35 patients at Hospital da Prelada (Porto, Portugal). Briefly, the skin tissue was cut in pieces of 0.5 by  
36 0.5 cm and incubated in a dispase solution (2.4 U.mL<sup>-1</sup> in PBS) at 4 °C overnight. After the tissue  
37 digestion, the epidermis was separated from the dermis, and the dermal pieces were digested  
38 overnight in a collagenase IA solution (125 U.mL<sup>-1</sup> in PBS) at 4 °C. Digestion products containing  
39 hDFbs were poured through a 100 µm cell strainer and centrifuged at 200 g for 5 minutes. The  
40 pellet was resuspended and the fibroblasts were subsequently cultured in Dulbecco's Modified  
41 Eagle Medium (DMEM) (Sigma, Germany) supplemented with 10% of fetal bovine serum (FBS,  
42 Gibco, UK) and 1% (v/v) antibiotic/antimycotic solution (A/B) (Gibco, UK) containing 100 units.mL<sup>-1</sup>  
43 penicillin and 100 mg.mL<sup>-1</sup> streptomycin, in a 37 °C humidified atmosphere with 5% CO<sub>2</sub>.  
44  
45  
46  
47  
48  
49  
50  
51  
52  
53  
54  
55  
56  
57  
58  
59  
60  
61  
62  
63  
64  
65

### ***Culture of hDFbs on the PA-HA membranes***

1 Membranes were prepared under sterile conditions as previously described. HA sterilization for  
2  
3 cell studies was done by dissolving the polymer in water, filtering the solution through a 0.22 µm  
4  
5 filter, followed by lyophilization in sterile falcon tubes (Sartorius, USA). PA solutions were sterilized  
6  
7 by UV exposure for 15 minutes. Confluent hDFbs were harvested from monolayer cultures using  
8  
9 TrypLE™ Express (Invitrogen, USA). Cells were seeded on the membranes ( $10^4$  cells.cm<sup>-2</sup>) and  
10  
11 cultured in DMEM supplemented with 10% FBS and 1% (v/v) A/B at 37 °C in a humidified  
12  
13 atmosphere of 5% CO<sub>2</sub> for 7 days. For inhibition studies, the cell culture media was supplemented  
14  
15 with 20 µM of GM6001 MMP-1 inhibitor (Chemicon, USA). Cell culture media was replaced twice a  
16  
17 week, and the collected conditioned media was stored frozen (-80 °C) until further analysis. At  
18  
19 predetermined time points, cell-cultured membranes were collected to assess cell proliferation  
20  
21 (DNA quantification), morphology and spreading (SEM, F-actin staining) and production of MMP-1,  
22  
23 collagen and ECM proteins. Cell culture experiments were performed in triplicate for each  
24  
25 condition and time point.  
26  
27  
28  
29  
30  
31  
32  
33  
34  
35  
36

### ***Cell proliferation***

37  
38 Cell proliferation was assessed at different culture times (1, 3 and 7 days) by quantifying the  
39  
40 amount of double-stranded DNA (dsDNA). Quantification was performed using the Quant-iT™  
41  
42 PicoGreen® dsDNA Assay Kit (Invitrogen, Molecular Probes, Oregon, USA), according to the  
43  
44 instructions of the manufacturer. Briefly, cells on the different membranes/coverslips were lysed  
45  
46 by osmotic and thermal shock and the supernatant used for the DNA quantification. The  
47  
48 fluorescent intensity of the dye was measured in a microplate reader (Synergie HT, Bio-Tek, USA)  
49  
50 with excitation at 485/20 nm and emission at 528/20 nm. The DNA concentration for each sample  
51  
52 was calculated using a standard curve (DNA concentration ranging from 0 to 1.5 mg/mL) relating  
53  
54  
55  
56  
57  
58  
59  
60  
61  
62  
63  
64  
65



1 quantity of DNA and fluorescence intensity. Three samples were analyzed per condition and time  
2 point.  
3  
4  
5

### 6 ***Staining and confocal microscopy*** 7

8  
9 For examination of cell morphology and MMP-1 production at the protein level, fibroblasts  
10 cultured on the different membranes/coverlips were stained for F-actin and MMP-1. Cells were  
11 washed in PBS and subsequently fixed in 10% formalin solution (Sigma-Aldrich, Germany) for 30  
12 minutes at 4 °C. Cells were then washed once with 0.1 M glycine in PBS and twice with PBS and  
13 permeabilized with 2% BSA/ 0.2% Triton X-100 solution for 1 h at RT. Samples were incubated with  
14 primary antibody anti-MMP-1 (ab38929, 1:100, abcam, UK) for 1 h at RT and washed three times  
15 for 2 minutes with PBS. Samples were then incubated with the secondary antibody, anti-mouse  
16 Alexa 488 (1:200, Molecular Probes, Invitrogen, USA) and TRITC-conjugated phalloidin (1 U/mL,  
17 Sigma-Aldrich, Germany) for 1 h at RT. Cell nuclei were counterstained with 1 mg/mL DAPI  
18 (1:1000, Sigma-Aldrich, Germany) for 10 min and washed with PBS. Visualization was performed  
19 by confocal laser scanning microscopy (CLSM, Olympus FluoView 1000, Olympus, Japan).  
20 Background was subtracted and images were processed using FV10-ASW 3.1 software (Olympus,  
21 Japan).  
22  
23  
24  
25  
26  
27  
28  
29  
30  
31  
32  
33  
34  
35  
36  
37  
38  
39  
40  
41  
42  
43  
44

### 45 ***Expression of MMP-1*** 46

47  
48 MMP-1 expression by hDFbs was evaluated by analyzing the conditioned medium collected from  
49 fibroblast cultures on the PA-HA membranes, or peptide-coated glass coverslips, at different  
50 culture times (1, 3 and 7 days). MMP-1 was quantified with a double sandwich enzyme-linked  
51 Immunosorbent assay (ELISA) kit (Human Total MMP-1 DuoSet, R&D Systems, USA) according to  
52 the instructions of the manufacturer. Optical density (OD) was read at 450 nm and 570 nm in a  
53 microplate reader (Synergie HT, Bio-Tek, USA). The MMP-1 concentration for each sample was  
54  
55  
56  
57  
58  
59  
60  
61  
62  
63  
64  
65

1  
2  
3  
4  
5  
6  
7  
8  
9  
10  
11  
12  
13  
14  
15  
16  
17  
18  
19  
20  
21  
22  
23  
24  
25  
26  
27  
28  
29  
30  
31  
32  
33  
34  
35  
36  
37  
38  
39  
40  
41  
42  
43  
44  
45  
46  
47  
48  
49  
50  
51  
52  
53  
54  
55  
56  
57  
58  
59  
60  
61  
62  
63  
64  
65

calculated using a standard curve relating quantity of MMP-1 and OD. Three samples were analyzed per condition and time point.

### ***Quantification of collagen and total ECM proteins***

The deposition of ECM proteins by hDFbs cultured on the different membranes was analysed by quantification of collagen and other non-collagenous proteins using a colorimetric analysis (Sirius red/Fast green collagen staining kit, Chondrex, USA) and following the instructions of the manufacturer.<sup>[50]</sup> Briefly, cells were washed in PBS and subsequently fixed in 10% formalin solution (Sigma-Aldrich, Germany) for 30 minutes at 4 °C. Cells were washed again in PBS and immersed in 200 µL of the dye solution containing Sirius red and fast green. The plates were incubated at RT for 30 minutes in a rotary shaker. The dye solutions were then carefully withdrawn, and the plates were washed repeatedly with distilled water until the solution was colorless. After washing, 1 mL of dye extraction solution was added to each sample to elute the color. Optical density (OD) was read at 540 nm and 605 nm in a microplate reader (Synergie HT, Bio-Tek, USA). The values of collagen and total ECM proteins were calculated following the manufacturer instructions and normalized to DNA content.

### **Data analysis and statistics**

All data values are presented as mean ± standard deviation (SD). Statistical analysis was performed using GraphPad Prism 5.00 software (San Diego, USA). Statistical differences between the different conditions (NAG, DNA, MMP-1 and collagenous/non-collagenous protein quantifications) were determined using a two-way analysis of variance (ANOVA) with a Bonferroni's multiple comparison post-hoc test (\*  $p < 0.05$ , \*\*  $p < 0.01$  and \*\*\* $p < 0.001$ ).

## References

- [1] M. Zelzer, S. J. Todd, A. R. Hirst, T. O. McDonald, R. V. Ulijn, *Biomaterials Science* 2013, 1, 11.
- [2] M. P. Lutolf, J. L. Lauer-Fields, H. G. Schmoekel, A. T. Metters, F. E. Weber, G. B. Fields, J. A. Hubbell, *Proceedings of the National Academy of Sciences* 2003, 100, 5413.
- [3] H. G. Schmoekel, F. E. Weber, J. C. Schense, K. W. Gratz, P. Schawalder, J. A. Hubbell, *Biotechnol Bioeng* 2005, 89, 253; A. H. Zisch, U. Schenk, J. C. Schense, S. E. Sakiyama-Elbert, J. A. Hubbell, *J Control Release* 2001, 72, 101.
- [4] K. B. Fonseca, F. R. Maia, F. A. Cruz, D. Andrade, M. A. Juliano, P. L. Granja, C. C. Barrias, *Soft Matter* 2013, 9, 3283.
- [5] S. Khetan, J. S. Katz, J. A. Burdick, *Soft Matter* 2009, 5, 1601.
- [6] S. Kim, K. E. Healy, *Biomacromolecules* 2003, 4, 1214; N. S. Khelfallah, G. Decher, P. J. Mésini, *Macromolecular Rapid Communications* 2006, 27, 1004.
- [7] P.-F. Caponi, X.-P. Qiu, F. Vilela, F. M. Winnik, R. V. Ulijn, *Polymer Chemistry* 2011, 2, 306; J. H. Collier, P. B. Messersmith, *Bioconjugate Chemistry* 2003, 14, 748; Z. Yang, M. Ma, B. Xu, *Soft Matter* 2009, 5, 2546; D. Koda, T. Maruyama, N. Minakuchi, K. Nakashima, M. Goto, *Chemical Communications* 2010, 46, 979.
- [8] H. W. Jun, V. Yuwono, S. E. Paramonov, J. D. Hartgerink, *Advanced Materials* 2005, 17, 2612; M. C. Giano, D. J. Pochan, J. P. Schneider, *Biomaterials* 2011, 32, 6471.
- [9] K. M. Galler, L. Aulisa, K. R. Regan, R. N. D'Souza, J. D. Hartgerink, *J Am Chem Soc* 2010, 132, 3217.
- [10] Y. Chau, Y. Luo, A. C. Y. Cheung, Y. Nagai, S. Zhang, J. B. Kobler, S. M. Zeitels, R. Langer, *Biomaterials* 2008, 29, 1713.
- [11] M. J. Webber, C. J. Newcomb, R. Bitton, S. I. Stupp, *Soft Matter* 2011, 7, 9665.
- [12] A. Dehsorkhi, I. W. Hamley, J. Seitsonen, J. Ruokolainen, *Langmuir* 2013, 29, 6665.
- [13] Y.-A. Lin, Y.-C. Ou, A. G. Cheetham, H. Cui, *Biomacromolecules* 2014, 15, 1419.
- [14] T. H. Vu, Z. Werb, *Genes & Development* 2000, 14, 2123; A. Page-McCaw, A. J. Ewald, Z. Werb, *Nat Rev Mol Cell Biol* 2007, 8, 221.
- [15] V.-M. Kähäri, U. Saarialho-Kere, *Experimental Dermatology* 1997, 6, 199.
- [16] S. V. Nolte, W. Xu, H. O. Rennekampff, H. P. Rodemann, *Cells Tissues Organs* 2008, 187, 165.
- [17] M. P. Lutolf, G. P. Raeber, A. H. Zisch, N. Tirelli, J. A. Hubbell, *Advanced Materials* 2003, 15, 888.
- [18] S. Werner, R. Grose, *Physiol Rev* 2003, 83, 835.
- [19] J. L. West, J. A. Hubbell, *Macromolecules* 1998, 32, 241.
- [20] J. Patterson, J. A. Hubbell, *Biomaterials* 2010, 31, 7836.
- [21] K. Bott, Z. Upton, K. Schrobback, M. Ehrbar, J. A. Hubbell, M. P. Lutolf, S. C. Rizzi, *Biomaterials* 2010, 31, 8454.
- [22] K. M. Galler, J. D. Hartgerink, A. C. Cavender, G. Schmalz, R. N. D'Souza, *Tissue Eng Part A* 2012, 18, 176.
- [23] J.-K. Kim, J. Anderson, H.-W. Jun, M. A. Repka, S. Jo, *Molecular Pharmaceutics* 2009, 6, 978; J. Banerjee, A. J. Hanson, B. Gadam, A. I. Elegbede, S. Tobwala, B. Ganguly, A. V. Wagh, W. W. Muhonen, B. Law, J. B. Shabb, D. K. Srivastava, S. Mallik, *Bioconjug Chem* 2009, 20, 1332.
- [24] J. Banerjee, A. J. Hanson, E. K. Nyren-Erickson, B. Ganguli, A. Wagh, W. W. Muhonen, B. Law, J. B. Shabb, D. K. Srivastava, S. Mallik, *Chem Commun (Camb)* 2010, 46, 3209.
- [25] K. T. Dicker, L. A. Gurski, S. Pradhan-Bhatt, R. L. Witt, M. C. Farach-Carson, X. Jia, *Acta Biomaterialia* 2014, 10, 1558; J. A. Burdick, G. D. Prestwich, *Advanced Materials* 2011, 23, H41.
- [26] A. Almond, *Cellular and Molecular Life Sciences* 2007, 64, 1591; T. C. Laurent, J. R. E. Fraser, *Faseb Journal* 1992, 6, 2397.
- [27] B. P. Toole, *Nature Reviews Cancer* 2004, 4, 528; M. A. Solis, Y.-H. Chen, T. Y. Wong, V. Z. Bittencourt, Y.-C. Lin, L. L. H. Huang, *Biochemistry research international* 2012, 2012, 346972.
- [28] M. David-Raoudi, F. Tranchepain, B. Deschrevel, J. C. Vincent, P. Bogdanowicz, K. Boumediene, J. P. Pujol, *Wound Repair Regen* 2008, 16, 274; R. A. Clark, K. Ghosh, M. G. Tonnesen, *J Invest Dermatol* 2007, 127, 1018; W. Y. Chen, G. Abatangelo, *Wound Repair Regen* 1999, 7, 79.
- [29] R. M. Capito, H. S. Azevedo, Y. S. Velichko, A. Mata, S. I. Stupp, *Science* 2008, 319, 1812.
- [30] D. S. Ferreira, A. P. Marques, R. L. Reis, H. S. Azevedo, *Biomaterials Science* 2013, 1, 952.

- [31] A. C. Mendes, K. H. Smith, E. Tejada-Montes, E. Engel, R. L. Reis, H. S. Azevedo, A. Mata, *Advanced Functional Materials* 2013, 23, 430.
- [32] J. D. Hartgerink, E. Beniash, S. I. Stupp, *Science* 2001, 294, 1684.
- [33] M. Ehrbar, S. C. Rizzi, R. G. Schoenmakers, B. S. Miguel, J. A. Hubbell, F. E. Weber, M. P. Lutolf, *Biomacromolecules* 2007, 8, 3000.
- [34] R. T. Aimes, J. P. Quigley, *Journal of Biological Chemistry* 1995, 270, 5872.
- [35] H. Nagase, G. B. Fields, *Biopolymers* 1996, 40, 399.
- [36] W. Babel, R. W. Glanville, *European Journal of Biochemistry* 1984, 143, 545.
- [37] N. Greenfield, G. D. Fasman, *Biochemistry* 1969, 8, 4108.
- [38] H. A. Behanna, J. J. Donners, A. C. Gordon, S. I. Stupp, *J Am Chem Soc* 2005, 127, 1193.
- [39] A. C. Mendes, E. T. Baran, R. L. Reis, H. S. Azevedo, *Wiley Interdisciplinary Reviews: Nanomedicine and Nanobiotechnology* 2013, 5, 582.
- [40] R. Langer, D. A. Tirrell, *Nature* 2004, 428, 487; L. G. Griffith, M. A. Swartz, *Nat Rev Mol Cell Biol* 2006, 7, 211; M. P. Lutolf, J. A. Hubbell, *Nature Biotechnology* 2005, 23, 47.
- [41] T. J. Shaw, P. Martin, *Journal of Cell Science* 2009, 122, 3209.
- [42] M. J. Webber, J. Tongers, M. A. Renault, J. G. Roncalli, D. W. Losordo, S. I. Stupp, *Acta Biomaterialia* 2010, 6, 3.
- [43] B. Martin-Martin, V. Tovell, A. H. Dahlmann-Noor, P. T. Khaw, M. Bailly, *Eur J Cell Biol* 2011, 90, 26.
- [44] Z. Werb, *Cell* 1997, 91, 439.
- [45] A. D. Widgerow, *Wound Repair Regen* 2011, 19, 117.
- [46] S. Werner, T. Krieg, H. Smola, *J Invest Dermatol* 2007, 127, 998; B. Hinz, *J Invest Dermatol* 2007, 127, 526.
- [47] O. Langholz, D. Rockel, C. Mauch, E. Kozłowska, I. Bank, T. Krieg, B. Eckes, *J Cell Biol* 1995, 131, 1903.
- [48] J. Varani, Y. Hattori, Y. Chi, T. Schmidt, P. Perone, M. E. Zeigler, D. J. Fader, T. M. Johnson, *Br J Cancer* 2000, 82, 657.
- [49] T. Takahashi, M. Ikegami-Kawai, R. Okuda, K. Suzuki, *Anal Biochem* 2003, 322, 257.
- [50] A. López-De León, M. Rojkind, *Journal of Histochemistry & Cytochemistry* 1985, 33, 737.

1 **Figure 1.** Design and characterization of the peptide amphiphiles (PAs) used in this study. (A) Chemical  
2 structure of the PAs showing the different functional segments. (B) Circular dichroism spectra of PA  
3 solutions (0.011 mM) at pH 3, 7, 9. (C) TEM images of PA nanostructures negatively stained with uranyl  
4 acetate (nanofibers were formed by the deposition of 0.1 wt% solutions in water followed by air drying on  
5 a carbon-coated TEM grid).  
6  
7  
8  
9

10  
11 **Figure 2.** Schematic illustration of the proposed enzyme-mediated degradation of self-assembled  
12 membranes made of hyaluronan (HA) and peptide nanofibers containing a cleavable site for MMP-1. The  
13 incorporation of a MMP-sensitive domain into the membrane design is expected to enhance their  
14 degradation by fibroblast secreted enzymes (HAase, MMP-1) and this would lead to enhance cellular  
15 invasion.  
16  
17  
18  
19

20  
21  
22 **Figure 3.** Degradation profile of the self-assembled membranes containing different functionalities. (A)  
23 Quantification of N-acetylamino sugars released from the membranes when incubated in PBS and in PBS  
24 containing 50 U/mL HAase, 10 nM human MMP-1 or both enzymes; Control (K<sub>3</sub>-HA, A1), MMP sensitive  
25 (MMP<sub>s</sub>K<sub>3</sub>-HA, A2) and MMP insensitive (MMP<sub>i</sub>K<sub>3</sub>-HA, A3) (\*p< 0.05, error bars represent standard deviation  
26 (n=3)). (B1) SEM images showing differences in membrane microstructure when exposed to enzyme  
27 solutions up to 14 days. (B2) Cross section of the MMP<sub>s</sub>K<sub>3</sub>-HA membranes after exposure to 10 nM MMP-1.  
28  
29  
30  
31  
32

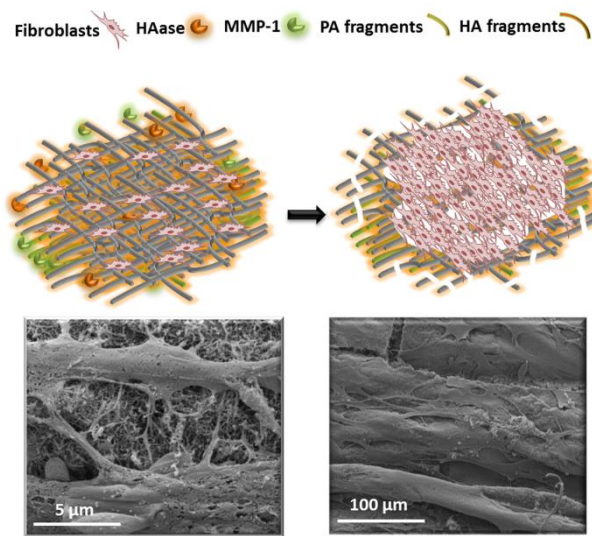
33  
34 **Figure 4.** Fibroblast proliferation when cultured on membranes with different functionalities. hDFb  
35 proliferation assessed by dsDNA quantification. (\*p< 0.05, error bars represent standard deviation (n= 3)).  
36  
37  
38

39  
40 **Figure 5.** Effect of membrane functionalization on the expression of MMP-1 by fibroblasts (hDFBs). (A)  
41 ELISA quantification of MMP-1 in cell culture supernatants (\*p< 0.05, error bars represent standard  
42 deviation (n= 3)). (B) Confocal microscopy images of fibroblasts stained for MMP-1 (green), F-actin (red)  
43 and nuclei (blue) after 24 hours.  
44  
45  
46  
47

48  
49 **Figure 6.** Concentration of ECM proteins, collagenous (A) and non-collagenous (B), secreted by hDFBs when  
50 cultured on the membranes with different functionalities (\*p< 0.05, error bars represent standard  
51 deviation (n= 3)).  
52  
53  
54

55  
56 **Figure 7.** SEM micrographs showing differences in membrane microstructure after culturing hDFBs for 14  
57 days, suggesting membrane cell-mediated degradation.  
58  
59  
60  
61

## Table of contents



**Self-assembling membranes, molecularly designed with enzyme-cleavable building blocks** (hyaluronan and peptide amphiphiles containing a proteolytic domain) afford cell-mediated degradation and leads to enhanced cellular colonization of the membranes. This concept can be used as a strategy to develop artificial matrices with more biomimetic degradation for tissue engineering applications.

Supporting Information

[Click here to download Supporting Information: adhm 201400586\\_Revised\\_SI\\_final.docx](#)

Figure 1

[Click here to download Production Data: Figure 1.tif](#)



Figure 2

[Click here to download Production Data: Figure 2.tif](#)

Figure 3

[Click here to download Production Data: Figure 3.tif](#)

Figure 4

[Click here to download Production Data: Figure 4.tif](#)

Figure 5

[Click here to download Production Data: Figure 5.tif](#)

Figure 6

[Click here to download Production Data: Figure 6.tif](#)

Figure 7

[Click here to download Production Data: Figure7.tif](#)

Image for Table of Contents

[Click here to download Production Data: GraphicalAbstract.tif](#)